Two Lipid Signals Guide Fruiting Body Development of *Myxococcus xanthus*

Swapna Bhat,[a] Tilman Ahrendt,[b] Christina Dauth,[b] Helge B. Bode,[b] Lawrence J. Shimkets[a]

Department of Microbiology, University of Georgia, Athens, GA, USA[a]; Merck Stiftungsprofessur für Molekulare Biotechnologie, Fachbereich Biowissenschaften, Goethe Universität Frankfurt, Frankfurt am Main, Germany[b]

ABSTRACT *Myxococcus xanthus* produces several extracellular signals that guide fruiting body morphogenesis and spore differentiation. Mutants defective in producing a signal may be rescued by codevelopment with wild-type cells or cell fractions containing the signal. In this paper, we identify two molecules that rescue development of the E signal-deficient mutant LS1191 at physiological concentrations, *iso*15:0 branched-chain fatty acid (FA) and 1-*iso*15:0-alkyl-2,3-di-*iso*15:0-acyl glycerol (TG1), a development-specific monoalkyl-diacylglycerol. The physiological concentrations of the bioactive lipids were determined by mass spectrometry from developing wild-type cells using chemically synthesized standards. Synthetic TG1 restored fruiting body morphogenesis and sporulation and activated the expression of the developmentally regulated gene with locus tag *MXAN_2146* at physiological concentrations, unlike its nearly identical tri-*iso*15:0 triacylglycerol (TAG) counterpart, which has an ester linkage instead of an ether linkage. *iso*15:0 FA restored development at physiological concentrations, unlike palmitic acid, a straight-chain fatty acid. The addition of either lipid stimulates cell shortening, with an 87% decline in membrane surface area, concomitantly with the production of lipid bodies at each cell pole and in the center of the cell. We suggest that cells produce triacylglycerol from membrane phospholipids. Bioactive lipids may be released by programmed cell death (PCD), which claims up to 80% of developing cells, since cells undergoing PCD produce lipid bodies before lysing.

IMPORTANCE Like mammalian adipose tissue, many of the *M. xanthus* lipid body lipids are triacylglycerols (TAGs), containing ester-linked fatty acids. In both systems, ester-linked fatty acids are retrieved from TAGs with lipases and consumed by the fatty acid degradation cycle. Both mammals and *M. xanthus* also produce lipids containing ether-linked fatty alcohols with alkyl or vinyl linkages, such as plasmalogens. Alkyl and vinyl linkages are not hydrolyzed by lipases, and no clear role has emerged for lipids bearing them. For example, plasmalogen deficiency in mice has detrimental consequences to spermatocyte development, myelination, axonal survival, eye development, and long-term survival, though the precise reasons remain elusive. Lipids containing alkyl- and vinyl-linked fatty alcohols are development-specific products in *M. xanthus*. Here, we show that one of them rescues the development of E signal-producing mutants at physiological concentrations.

Address correspondence to Lawrence J. Shimkets, shimkets@uga.edu.

Myxococcus xanthus responds to amino acid deprivation by inducing a multicellular developmental cycle that culminates in spore-filled fruiting bodies. While triacylglycerols (TAGs) and the related monoalkyl-diacylglycerols are relatively rare in prokaryotes, lipid bodies containing these neutral lipids are produced during *M. xanthus* development (1, 2). *M. xanthus* lipid bodies are surrounded by a monolayer phosphatidylethanolamine membrane containing an alkyl- or vinyl-linked fatty alcohol (1). As limited carbon and energy induce development (3, 4), it remains unclear what resources contribute to lipid body production.

Fruiting body development leads to differentiation of three distinct cell types, peripheral rods, myxospores, and cells that undergo programmed cell death (PCD) (5–7). Peripheral rods remain outside the fruiting body and seem to express different genes than sporulating cells (1, 5). They fail to produce lipid bodies (1).

PCD and sporulation occur inside the fruiting body. PCD begins approximately 12 h after initiation and claims up to 80% of the cell population (6–8). The mechanism and role of PCD remains unknown (9, 10).

A variety of extracellular signals are thought to guide morphogenesis, since many developmental mutants can be rescued for sporulation by codevelopment with wild-type cells or mutant cells belonging to a different complementation group (11). In most cases, the signaling molecules remain unknown. The E signal complementation group is attractive for signal identification since mutations that block E signal production also block the synthesis of isovaleryl-coenzyme A (CoA), the primer used for *iso*15:0 fatty acid (FA) biosynthesis and the production of certain secondary metabolites. Isovaleryl-CoA is synthesized by two pathways in *M. xanthus*. The first pathway uses branched-chain keto acid dehydrogenase (Bkd) to produce isovaleryl-CoA from leucine (12).

The second pathway produces isovaleryl-CoA by a novel mechanism involving LiuC, MvaS, MXAN_4264, MXAN_4265, and MXAN_4266 (13–15). Isovaleryl-CoA is extended by fatty acid synthase into *iso*15:0 and *iso*17:0 FAs.

E signal mutants exhibit incomplete aggregation and produce few spores (12, 16, 17). E signal mutants can be restored for aggregation and sporulation when allowed to develop atop agar containing 1 mM isovalerate or 1 mM *iso*15:0 FA, suggesting that *iso*15:0 FA or a molecule containing it may be the E signal (2). In addition, certain molecules containing *iso*15:0 FA, such as the monoalkyl-diacylglycerol TG1 (1-*iso*15:0-alkyl-2,3-di-*iso*15:0-acyl glycerol), also rescue aggregation and sporulation when placed on a lawn of cells (2). These experiments provide tantalizing evidence that certain lipids may be signaling molecules but stop short of proving the point, since excessive lipid concentrations were used and the metabolism of these molecules could generate other compounds.

We approached signal identification from a traditional biochemical standpoint by purifying bioactive molecules that restore E signal mutant development. Our data indicate that *iso*15:0 FA and TG1 are developmental signals that stimulate development when presented extracellularly at physiological concentrations. Lipid body synthesis begins before cells commit to PCD, and we suggest that cells undergoing PCD release these lipids into the fruiting body.

RESULTS

Bioactive molecules were extracted with chloroform and methanol 24 h after initiation of the development of *M. xanthus* strain DK5614, which exhibits normal development and is highly enriched in branched-chain fatty acids (18). Purification by solid-phase extraction on silica gel produced five fractions representing the major *M. xanthus* lipid classes (19). The activity of each fraction was quantified using a bioassay involving the restoration of sporulation to the E signal-deficient mutant LS1191 (*esg MXAN_4265*). LS1191 is unable to synthesize isovaleryl-CoA by either pathway and is consequently unable to synthesize *iso*15:0 and *iso*17:0 branched-chain fatty acids. Lipids dissolved in chloroform/methanol (2:1) were applied to Whatman filter paper disks. The filter disks were dried and then applied to LS1191 cells undergoing development. During a 4-day incubation period, cells swarm on to the disks and form myxospores if a stimulatory lipid is present. Cells were killed by heat treatment, and spores on the filter disks were germinated on nutrient-rich CYEK medium (9). After 24 to 48 h of incubation, swarms of cells migrated away from the filter paper disks. Swarming is a social behavior, and the rate of swarm expansion is directly proportional to the cell number (20). In our assay, swarm expansion is used as a proxy for spore number. Swarm expansion increases with lipid concentration over a broad range of concentrations, reflecting improved sporulation with increasing amounts of lipid (Fig. 1A). The metric used for comparing the bioactivity of each lipid fraction is the lipid amount per disk that caused half-maximal swarm expansion (half-maximal concentration), calculated from a plot of lipid concentration versus swarm expansion.

Fraction 1 was the most active fraction, with a half-maximal concentration of 2.3 µg/disk, representing a 43.5-fold purification from the lipid extract (Fig. 1B). Lipids in this fraction were further separated by silica gel thin-layer chromatography resolved with chloroform/cyclohexane (1:1), which produced five lipid spots
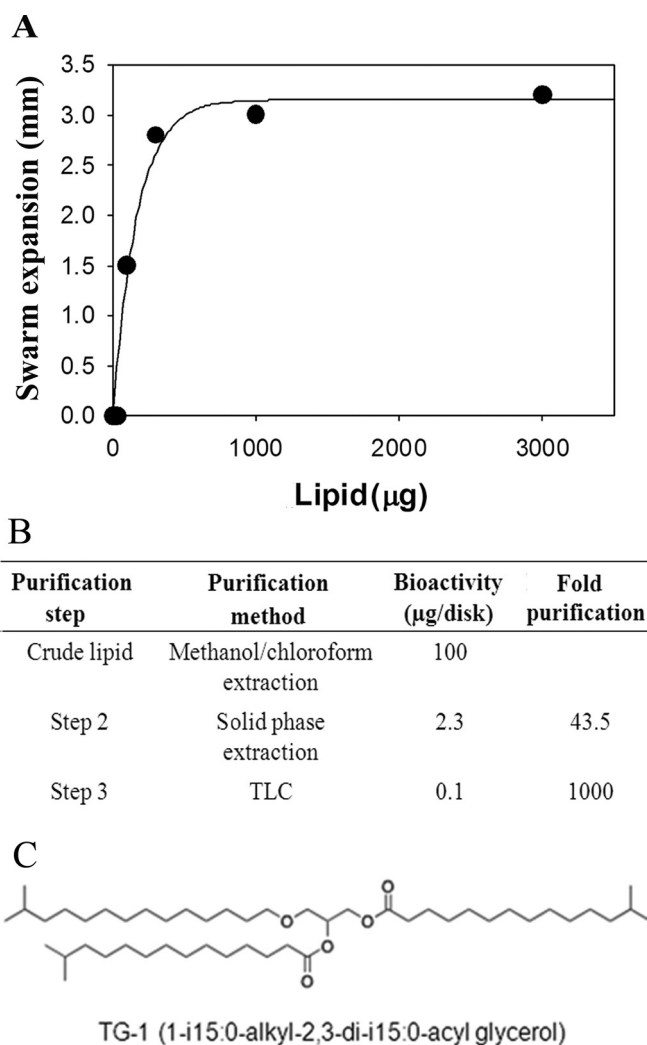

FIG 1 Purification of the E signal. (A) An example of a plot of lipid amount per disk versus swarm distance. (B) Purification of E signal activity. Bioactivity refers to lipid concentration giving half-maximal swarm expansion. (C) Chemical structure of TG1, the principal TAG in fraction 1.

that were visualized by staining with iodine. Lipid from only one spot, R_f (distance from start to center of substance spot divided by distance from start to solvent front) 0.4, rescued sporulation of LS1191. The half-maximal concentration was 100 ng/disk, representing an overall 1,000-fold purification (Fig. 1B).

Matrix-assisted laser desorption-ionization--time of flight (MALDI-TOF) mass spectrometry was used to identify lipids in the active fraction following thin-layer chromatography (TLC). An extensive catalog of lipid structures exists from previous work. The major peak is the ether lipid, TG1 (see Fig. S1, peak 773.7, in the supplemental material) (1, 2). TG1 contains one alkyl ether-linked *iso*15:0 fatty alcohol and two ester-linked *iso*15:0 fatty acids (Fig. 1C). The second largest signal was obtained from a closely related ether lipid containing *iso*17:0 fatty acid rather than *iso*15:0 fatty acid at the *sn*-2 position (Fig. S1, peak 801.7). Given the discovery of TG1 in this fraction, this result is not unexpected, since *iso*17:0 FA is synthesized via the same pathway and is the second most abundant branched-chain fatty acid (21).
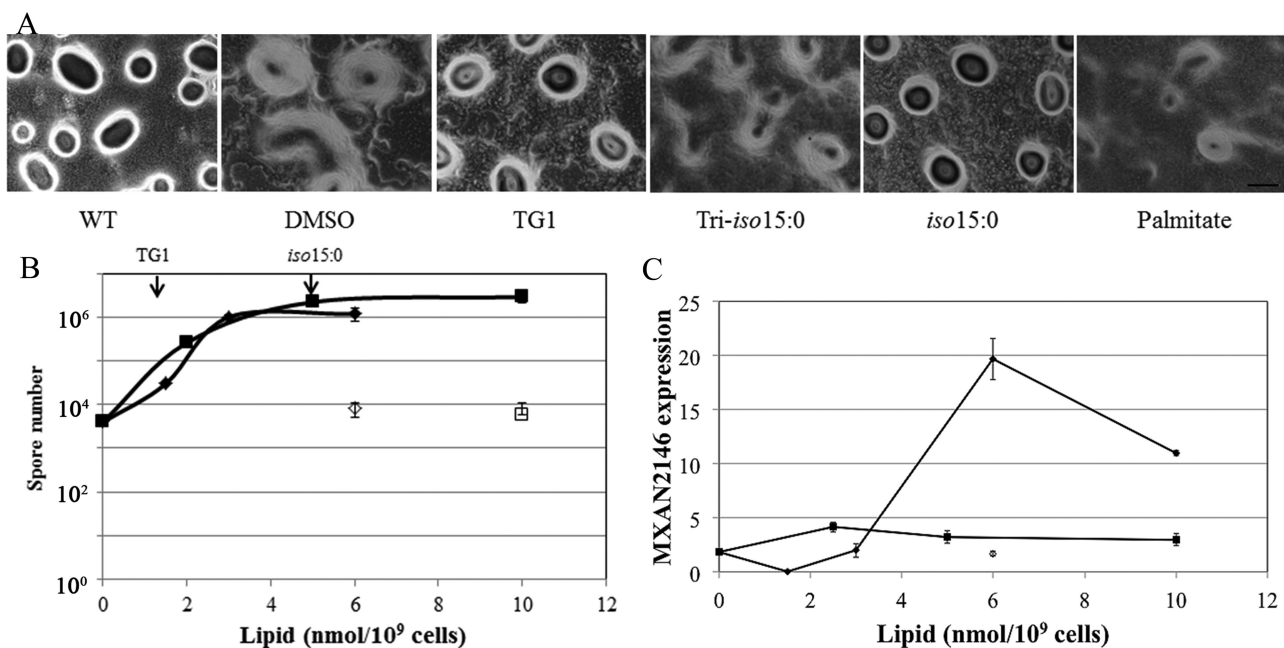
FIG 2 Rescue of development with synthetic lipids. (A) Fruiting body formation of wild-type (WT) strain DK1622 and of strain LS1191 mixed with DMSO, TG1 (3 nmol/10^9 cells), tri-*iso*15:0 TAG (3 nmol/10^9 cells), *iso*15:0 FA (5 nmol/10^9 cells), and palmitate (10 nmol/10^9 cells). Bar is 100 μm. (B) Heat- and sonication-resistant LS1191 spores were counted using a Petroff Hausser counting chamber following treatment with TG1 (◆), *iso*15:0 FA (■), tri-*iso*15:0 TAG (◇), and palmitic acid (□). Vertical arrows indicate physiological concentrations of TG1 and *iso*15:0 FA. (C) Quantitative PCR analysis of the expression levels of MXAN_2146 in LS1191 cells mixed with TG-1 (◆), *iso*15:0 FA (■), and tri-*iso*15:0 TAG (◇) at 24 h during development. Error bars show standard deviations.

Fraction 2, enriched in ester-linked triglycerides, was 200-fold less active than fraction 1, with a half-maximal concentration of 450 μg, and was not fractionated further. The principal TAG in this fraction is tri-*iso*15:0 TAG, which is identical to TG1 except that it has three ester-linked *iso*15:0 fatty acids. Since the only difference between this molecule and TG1 is the presence of the ether linkage, tri-*iso*15:0 TAG was synthesized and used in subsequent experiments to assess the importance of the ether linkage. Fraction 3, free fatty acids, had a half-maximal concentration of 5 μg. *iso*15:0 FA accounted for 65% of the branched-chain fatty acids in this fraction, though there were many other components. Fraction 4, enriched in mono- and diacylglycerides, and fraction 5, enriched in phospholipids, had half-maximal-concentration values of 87 μg and 2,300 μg, respectively, and were not fractionated further.

TG1, the major TAG in fraction 1, tri-*iso*15:0 TAG, the major TAG in fraction 2, and *iso*15:0 FA, the major fatty acid in fraction 3, were synthesized and assayed for sporulation rescue of LS1191 using the same bioassay. The half-maximal concentration for bioactivity of synthetic TG1 was 50 ng (66 pmol/disk), about 2-fold greater than that of the purified lipid fraction containing TG1. For comparison, tri-*iso*15:0 TAG was inactive in amounts as high as 3 μg/disk (half-maximal concentration of >4.0 nmol/disk). The half-maximal concentration of *iso*15:0 FA was 10 ng (41 pmol/disk).

Quantification of TG1 and *iso*15:0 FA. To ascertain whether TG1 and *iso*15:0 FA were active at physiological concentrations, both lipids were quantified in vegetative and 18-h developing wild-type cells (DK1622). Because lipids are largely insoluble in aqueous environments, the reagents used to quantitatively extract lipids, such as chloroform and methanol, are lethal. Thus, it was

not feasible to quantify intracellular versus extracellular lipids in a dense biofilm of developing cells, and for that reason, total lipid was extracted with chloroform/methanol (2:1).

Calibration curves for quantitative analysis were constructed using TG1 and *iso*15:0 FA standards. TG1 was not detected in vegetative cells (<0.004 nmol/10^9 cells) but increased to 1.4 nmol/10^9 cells by 18 h. Free *iso*15:0 fatty acid was 4.5 nmol/10^9 cells in both vegetative and 18-h developing cells. Total *iso*15:0 FA was determined following methanolysis of all lipids to release fatty acid methyl esters. The total amount of *iso*15:0 FA was 63.5 nmol/10^9 vegetative cells, which increased to 82.7 nmol/10^9 cells by 18 h. Thus, free *iso*15:0 FA represented about 5% of the total.

Developmental rescue by physiological concentrations of TG1 and *iso*15:0 FA. The precise number of cells that swarmed onto each filter paper disk in the bioassay was difficult to determine due to the porosity of the filters. Each disk was placed atop a spot containing 2.5×10^7 cells. This number provided a metric for comparison, assuming that most cells responded to the lipid. With *iso*15:0 FA, the half-maximal concentration was 41 pmol/disk or 1.6 nmol/10^9 cells. This was about one-third of the actual *iso*15:0 FA concentration. The half-maximal concentration of TG1 was 66 pmol/disk or about 2.6 nmol/10^9 cells. This was about 2-fold higher than the actual concentration. Thus, both molecules appeared to be active at or near their physiological concentrations.

A nontoxic lipid delivery system was developed so that the lipid concentration per cell could be carefully controlled. Lipid was dissolved in dimethyl sulfoxide (DMSO) and mixed with vegetative LS1191 cells. The cells were spotted on TPM agar plates under normal developmental conditions (9). The presence of DMSO alone had little effect on LS1191 development. The cells formed loose aggregates without spores, just like LS1191 without DMSO

(Fig. 2A and data not shown). TG1 restored fruiting body development at physiological concentrations, whereas at comparable concentrations, tri-*iso*15:0 TAG did not. Similarly, *iso*15:0 FA restored fruiting body development at physiological concentrations, whereas palmitate, a 16:0 straight-chain fatty acid of similar length and saturation, did not.

Spore yield was determined by direct counts following sonication to disperse spores and lyse vegetative cells. *iso*15:0 FA induced wild-type levels of spores (about 2.5×10^6 for wild-type strain DK1622) at physiological concentrations. However, unlike DK1622, which enjoyed a 75% germination rate after heating to 50°C for 2 h, only about 36% of the *iso*15:0 FA-induced spores germinated. TG1 had activity similar to that of *iso*15:0 FA at comparable concentrations (Fig. 2B), but the germination success was about 71%. Chemical specificity was observed in that the closely related molecules palmitate and tri-*iso*15:0 TAG were inactive at similar concentrations.

Physiological changes caused by TG1 and *iso*15:0 FA. The search for targets of the lipids focused on two areas, regulation of gene expression and induction of cell shape change. Published microarray data helped identify genes whose expression peaks during spore formation (22). The C signal-dependent aqualysin-like gene *MXAN_1501* that is activated at about 14 h (23–25) is not activated by either lipid. However, TG1 stimulated *MXAN_2146* expression, whereas neither *iso*15:0 FA nor tri-*iso*15:0 TAG induced expression (Fig. 2C). There are no features of the *MXAN_2146* promoter region that provide a clue about the mechanism of regulation.

DK1622 (wild-type) cells 18 h into the developmental program generally contain 2 to 3 large lipid bodies that comprise a substantial portion of the cell volume (1). As development is induced by carbon limitation, a relevant question is where the carbon and energy for lipid body production originate. Myxospore differentiation is an encystment in which cylindrical cells that are about 7 μm in length and 1 μm in width shorten into spherical spores that are roughly 1.8 μm in diameter. Excluding the thick cortex and spore coat layers, the diameter of the spore interior surrounded by the membrane is about 1 μm (26). The membrane surface area of the cylindrical cell, 23.6 μm^2, declines to 3.1 μm^2 in a spore, a decrease of 87%. On theoretical grounds, membrane phospholipid could serve as the principal carbon source for TAGs, with little biochemical complexity to the conversion and little drain on limiting carbon resources.

LS1191 cells are blocked early in development, before there is any indication of cell shortening or lipid body synthesis (Fig. 3A). When LS1191 cells were mixed with either TG1 or *iso*15:0 FA and spotted on TPM agar, lipid bodies were detected in most cells by 12 h (Fig. 3A). The sporulating cells became spindle shaped and produced lipid bodies in the center of the cell and at both poles. The solvent used to dissolve the lipids, DMSO, did not induce lipid body production (Fig. 3A), nor did the closely related compounds tri-*iso*15:0 TAG or palmitate (not shown). In the case of *iso*15:0 FA, maximum lipid body production is observed at physiological concentrations (Fig. 3B, vertical arrow). TG1 produces only about 1/3 the maximum level of lipid bodies at the average physiological concentration and normal levels at a 3-fold-higher concentration. Neither tri-*iso*15:0 TAG nor palmitate stimulated lipid body production (Fig. 3B; see also Fig. S2 in the supplemental material).

We noted several striking differences between wild-type devel-

opment and *iso*15:0 FA-rescued sporulation of LS1191 cells. Whereas wild-type cells also tend to have lipid bodies at each pole and in the cell center, there is more variation in lipid body size and spatial location (1). In contrast, *iso*15:0 FA-induced lipid bodies appear to be larger and more precisely located in LS1191 cells. The central lipid bodies are so large that the cells adopt more of a spindle shape than wild-type cells. In addition, *iso*15:0 FA-rescued development results in balloon-shaped outer membrane blebs protruding from the cell surface in over 50% of the cells. This result suggests that *iso*15:0 FA diminishes cell length faster than the natural rate of outer membrane sloughing. As the wild-type cells become shorter, the outer membrane disappears gradually, without any obvious distortion to the cell surface (1). Secretion of outer membrane material through outer membrane vesicles or by TraAB-mediated intercellular exchange is in each case a well-documented, natural venue for diminishing the outer membrane in wild-type cells (27–29). It appears as if *iso*15:0 FA uncouples outer membrane sloughing from lipid body synthesis to generate these unusual structures.

When LS1191 cells were mixed with *iso*15:0 FA and induced to develop, the cell length diminished as the lipid body area increased (Fig. 3C). The delivery solvent DMSO alone did not alter either parameter significantly. A concomitant decline in cell length as the lipid body area increased was also observed during wild-type development (not shown), suggesting that excess membrane phosphatidylethanolamine (PE) is converted to triacylglycerides during shortening.

Cells undergoing PCD produce lipid bodies. Both *iso*15:0 FA and TG1 stimulate development from the outside in, suggesting that the lipids are normally presented extracellularly. Where do they come from? Because of the complex structure of the cell envelop, it seems unlikely that lipid bodies are secreted. A more likely venue for lipid release from the cell is through PCD, which is the fate of 80% of the population. We examined the possibility that PCD generates extracellular lipid by determining whether cells destined for PCD form lipid bodies.

Nile red staining was used to quantify lipid body-producing cells during wild-type development. At 12 h, nearly 90% of the cells contained lipid bodies (Fig. 4A). Peripheral rods, which comprise 10% of the population, do not make lipid bodies and account for the difference (1). Over the course of development, the cell number declined roughly 80% due to PCD and was accompanied by a corresponding decline in the number of cells containing lipid bodies (Fig. 4A). These results suggest that cells destined for PCD produce lipid bodies.

This observation was examined in a different manner by using a pair of strains in which one member preferentially undergoes PCD. Δ*difA* cells, formerly called *dsp* in the older literature, undergo PCD when mixed with DK1622 cells (8, 30). In these experiments, the Δ*difA* mutant expressed green fluorescent protein to provide a cell type-specific marker (see Fig. S2 in the supplemental material). When allowed to develop alone, Δ*difA* cells failed to undergo either PCD or sporulation (Fig. 4B). While lipid body synthesis and cell shortening were delayed relative to these processes in wild-type cells, the majority of the cells eventually produced lipid bodies.

The two strains were mixed 1:1 and allowed to develop. Cells were stained with Nile red every 12 h and examined for red and green fluorescence. Overall, Δ*difA* cells declined by over 90% by 48 h (Fig. 4C). While the production of lipid bodies by Δ*difA* cells
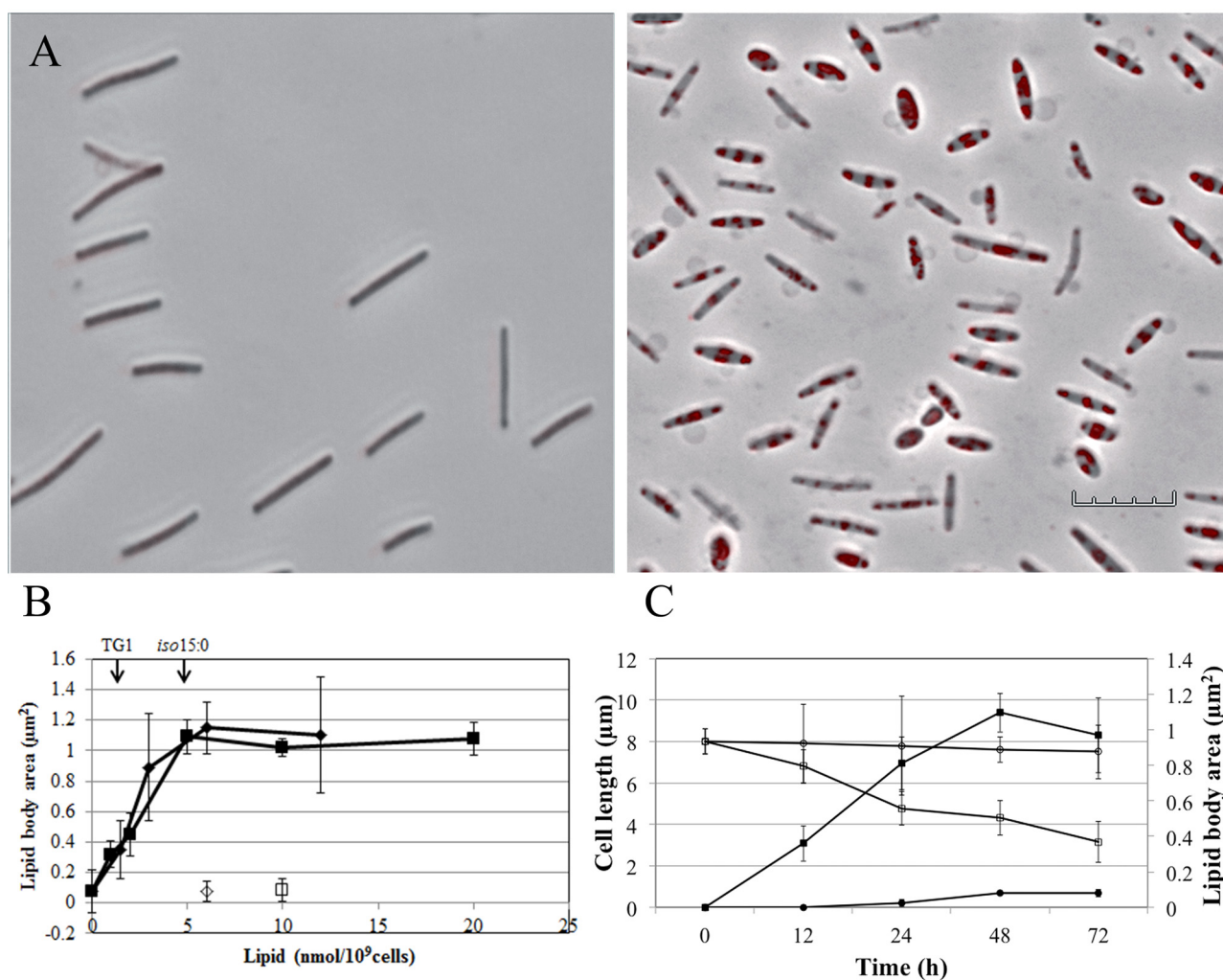
FIG 3 Rescue of development by synthetic lipids. (A) Lipid body production in LS1191 mixed with DMSO (left) and DMSO plus *iso*15:0 FA (right). (B) Lipid body production at 48 h was quantified by measuring the average area of lipid bodies per 30 cells following treatment with *iso*15:0 FA (■), TG1 (♦), tri-*iso*15:0 TAG (◇), and palmitic acid (□). Vertical arrows indicate physiological concentrations of TG1 and *iso*15:0 FA. (C) Lipid body production increases as cell length diminishes. LS1191 lipid body area was quantified after mixture with DMSO (●) or DMSO plus 5 nmol *iso*15:0 FA/10^9 cells (■). Cell length was measured using phase-contrast images of 30 rod-shaped cells of LS1191 mixed with DMSO (○) or DMSO plus 5 nmol *iso*15:0 FA/10^9 cells (□). The same cells were measured for length and lipid body production. Error bars show standard deviations.

was still delayed relative to the lipid body production of wild-type cells (Fig. 4C), the number of Δ*difA* cells containing lipid bodies initially increased and then declined steadily after 24 h. Δ*difA* cells formed only 0.1% of the spore population. These results show that cells undergoing PCD produce lipid bodies. As Δ*difA* cells did not undergo PCD on their own, it appears as if wild-type cells stimulate Δ*difA* PCD.

PCD would be expected to release lipid bodies inside the fruiting body. When fruiting bodies were stained with Nile red and then gently opened in the presence of Ficoll to stabilize the cell membrane, spherical bodies containing lipid were observed (see Fig. S3 in the supplemental material). The spherical bodies exhibited a range of sizes, many with diameters smaller than the 2.5-μm spore diameter. Furthermore, the ones shown in the right panel of Fig. S3 were nonrefractile under phase-contrast microscopy, suggesting that they were membrane vesicles.

DISCUSSION

Novel lipid signals. We describe two novel bioactive lipids for *M. xanthus*, *iso*15:0 fatty acid (FA) and the TAG TG1. We tentatively refer to them as signals because they are active from the outside in at physiological concentrations, though sensory pathways have not yet been identified. *iso*15:0 FA exhibited full activity at its physiological concentration in all but the gene expression assay. TG1 exhibited roughly 30% activity at its average physiological concentration and full activity at 3-fold-higher concentrations. As *iso*15:0 FA is a precursor for TG1 synthesis and TG1 can be partially catabolized to *iso*15:0 FA, the question arises whether only one of these lipids is the actual E signal. TG1 could do everything *iso*15:0 FA could plus activate the expression of the spore-specific gene *MXAN_2146*. Its unusual chemical structure, production only during development, and activity at low concentrations argue in favor of TG1 being a developmental sig-
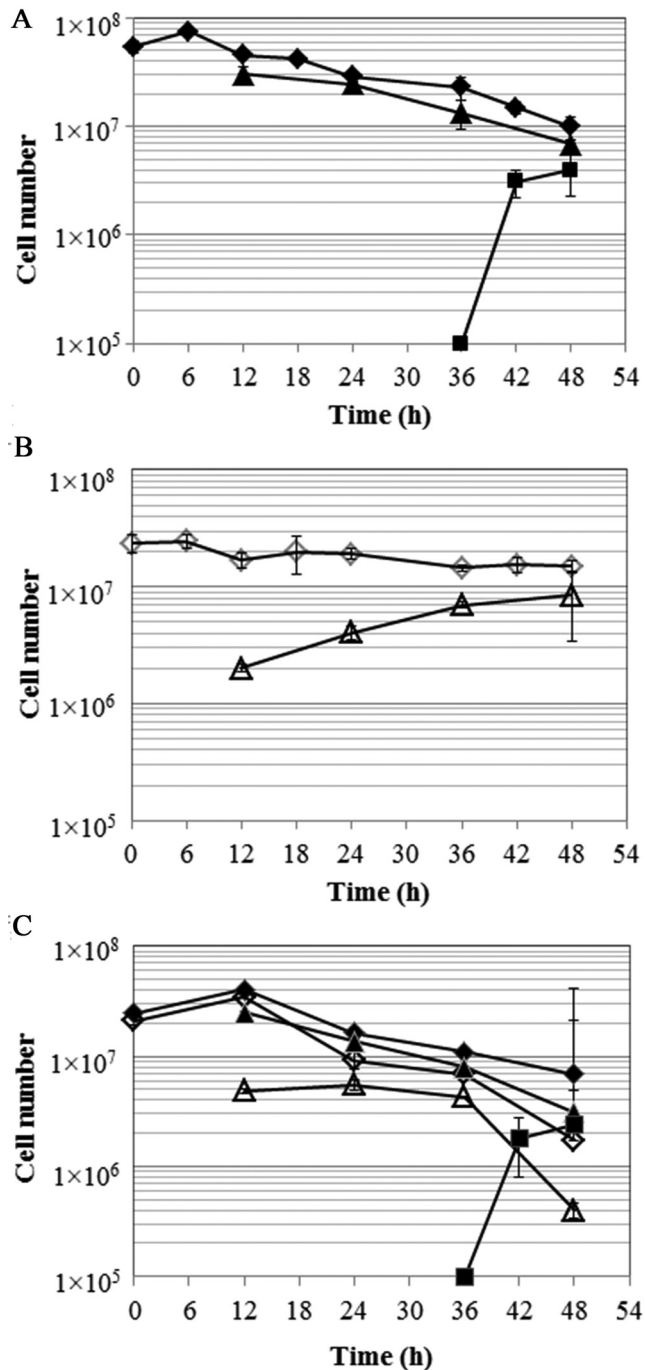
FIG 4 Lipid body production in WT, Δ*difA*, and WT plus Δ*difA* cells during development. (A) Changes in WT cell number during development as determined by direct counts of rod-shaped cells (◆), myxospores (■), and lipid body-containing cells, which were enumerated by Nile red staining (▲). (B) Changes in LS2472 (Δ*difA* P$_{pilA}$-*gfp*) cell numbers and lipid body-containing cells as shown by counts of rod-shaped cells (◇) and lipid body-containing cells (Δ). (C) Changes in WT and LS2472 cell numbers when mixed 1:1 and allowed to develop. LS2472 cells were identified using green fluorescence. Lipid body-containing cells were identified by Nile red staining. Symbols are as indicated for panels A and B. Error bars show standard deviations.

nal. It seems unlikely that the biological activity of TG1 is due to catabolism to *iso*15:0 FA, as tri-*iso*15:0 TAG was at least 60-fold

less active than TG1 despite having a similar catabolic pathway. When dose-response curves are carefully compared, a case can also be made for *iso*15:0 FA being a signal. As it takes 3 molecules of *iso*15:0 FA to form one molecule of TG1, it should take three times the amount of *iso*15:0 FA to restore development if the *iso*15:0 FA activity is due to TG1 production. In both the lipid body production assay (Fig. 3B) and the sporulation assay (Fig. 2B), the active concentration of *iso*15:0 FA was roughly equal to that of TG1. The slopes of the activity curves were comparable, as were the lipid amounts per disk that caused half-maximal swarm expansion (half-maximal concentration) and the concentrations required for maximum activity. The easiest way to reconcile the results is by arguing that *iso*15:0 FA and TG1 have partially overlapping functions. Some features of the chemical structures that confer activity were revealed. Palmitate could not replace *iso*15:0 FA despite having a similar chain length and saturation. This argues for the importance of the *iso* branch in initiating the developmental response. Similarly, tri-*iso*15:0 TAG could not replace TG1 despite being identical except for the alkyl ether linkage in TG1. Ether lipids are rare in the *Bacteria*, and this is the first report of one serving as a signaling molecule.

Both lipids are active when presented extracellularly either on a filter paper disk or dissolved in DMSO. Lipid bodies are not likely to pass directly through the multilayered cell envelope. Rather, they are produced by cells destined for PCD (Fig. 4) and released into the fruiting body (see Fig. S3 in the supplemental material). Since the vast majority of the cells undergo PCD, these cells would produce quantities sufficient to activate morphogenesis. While PCD has long been thought to deliver vital nutrients to developing cells, our work indicates that it also provides essential developmental signals (7).

As development is initiated when cells encounter limiting carbon and energy resources, it would appear that lipid bodies are made from existing resources. This would suggest an internal source for lipid body fatty acids. Our work demonstrates that lipid bodies are produced when cells begin to shorten and are first observed about 6 h after the initiation of development in wild-type cells. The membrane surface area diminishes roughly 87% during development. Since we show that cell shortening and lipid body production are coupled processes, TAGs could be produced from membrane phospholipid in a direct and simple manner (Fig. 5). The model proposes that the inner leaflet of the inner membrane forms the monolayer membrane surrounding the lipid body, as has been described for lipid bodies from other organisms (31). The principal phospholipid in both membranes is phosphatidylethanolamine (PE) (1, 2, 32), though some chemical modifications must be made. Vegetative PE contains two ester-linked fatty acids, while lipid body PE contains one alkyl- or vinyl-linked fatty alcohol. The outer leaflet of the inner membrane would be used to create triglycerides from phospholipids in two enzymatic steps. In the first step, the phosphorylated head group of the phospholipid is removed to create diacyl glycerol. In the second step, diacylglycerol acyltransferase produces triacylglycerol. The mechanism by which *iso*15:0 FA and TG1 activate this pathway remains unknown. They could activate transcription of the relevant genes or modulate the activity of existing enzymes.

The peptidoglycan layer and outer membrane must also shrink, as the membrane surface area declined by 87%. The peptidoglycan sacculus is degraded during the transition from vegetative cells to glycerol-induced myxospores (33). The spherical
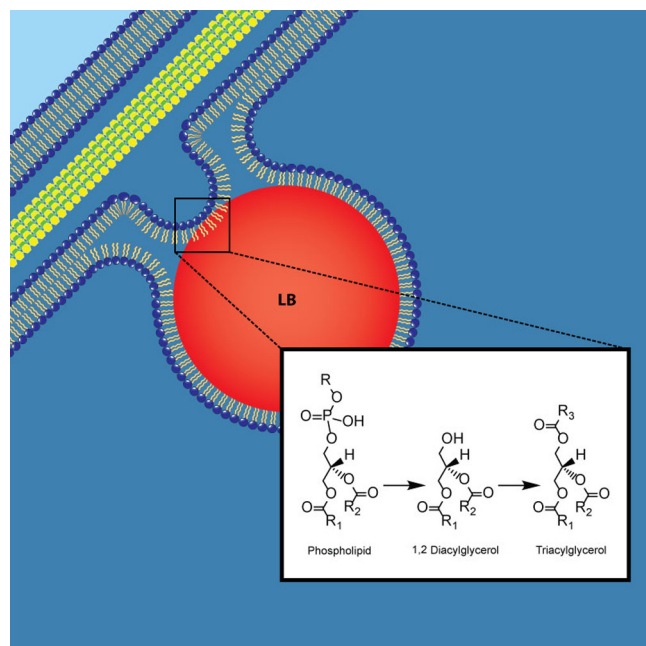
FIG 5 Model for conversion of membrane phospholipids into triacylglycerides in lipid bodies. The model proposes that the inner leaflet of the inner membrane forms the monolayer membrane surrounding the lipid bodies (LB), as has been described for lipid bodies from other organisms. The principal phospholipid in both membranes is phosphatidylethanolamine (PE) (2, 11, 32), though some chemical modifications must be made. Vegetative PE contains ester-linked fatty acids, while lipid body PE contain one alkyl- or vinyl-linked fatty alcohol. We propose that the outer leaflet of the inner membrane would be used to create triglycerides from phospholipids in two enzymatic steps. First, the phospho head group is removed to create a diacylglyceride. Then, an acyl chain is added by an acyl transferase to create the triacyglyceride.

coats isolated from glycerol-induced spores contain no detectable muropeptides but do have small amounts of *N*-acetylmuramic acid and *meso*-diaminopimelic acid. Fruiting body spores have not been examined in the same detail. The outer membrane sloughs off normally by several mechanisms, principally by the formation of outer membrane vesicles and cell contact-dependent exchange between cells (27, 28, 34).

MATERIALS AND METHODS

Bacterial strains and growth conditions. Details about cultivation, development, and strain construction are provided in Text S1 and Table S1 in the supplemental material.

Nile red staining. Lipid body staining was carried out as described by Hoiczyk et al. with modifications (1). Detailed information on lipid body staining and microscopy is provided in Text S1 in the supplemental material.

Filter paper disk lipid bioassay. Lipid fractions and synthetic lipids were assayed for their ability to rescue sporulation of LS1191. Cells were grown to a density of 5×10^8 cells/ml, harvested, and resuspended in distilled water to a final density of 5×10^8 cells/ml. Amounts of 50 μl of cells were spotted on TPM plates, allowed to air dry and incubated at 32°C for 24 h. Lipid amounts ranging from 0 to 10 μg were applied to sterile circular Whatman number 2 filter paper disks (7 mm), dried, and then placed on top of cell spots. The plates were incubated for 96 h at 32°C. The plates were incubated at 50°C for 2 h to kill vegetative cells. The plates were cooled, and the filter disks were then transferred to CYEK plates. The plates were incubated for 24 to 48 h until swarms of cells appeared around

the filter disk. The swarm sizes at five equidistant points were recorded using a phase-contrast microscope (Leitz Laborlux) with an ocular micrometer. The average swarm size was plotted against the lipid concentration.

Lipid-DMSO bioassay. Synthetic lipids were utilized for bioassays involving lipid delivery in DMSO. LS1191 cells were grown to a density of 5×10^8 cells/ml, harvested, and concentrated to a final density of 5×10^9 cells/ml. Lipids were dissolved in 100% DMSO at 0.6 nmol/μl and diluted in 100% DMSO. Lipids were added to LS1191 cells, and amounts of 10 μl of cell suspension were spotted onto TPM plates. The plates were incubated at 32°C.

Real-time PCR. To quantify the mRNA levels of MXAN_2146, total RNA was extracted using RNA*snap* (*s*imple *n*ucleic *a*cid *p*urification) from LS1191 mixed with different lipids at 24 h into development. Primers for reverse transcription (RT)-PCR are provided in Table S1 in the supplemental material. Quantification of transcript levels was done using the iScript one-step RT-PCR with SYBR green (Bio-Rad, Hercules, CA, USA) and carried out with the iCycler iQ real-time PCR detection system (Bio-Rad, Hercules, CA, USA) with the following reaction cycle: 50°C for 10 min, 95°C for 5 min, and then 45 cycles of 95°C for 10 s, 55°C for 30 s, and 72°C for 30 s. Melting curve analysis was carried out at 55 to 95°C for 10 s, increasing the temperature 0.5°C each cycle for 80 cycles. Relative fold changes in MXAN_2146 transcript levels were calculated using the cycle threshold ($\Delta\Delta C_T$) method.

Lipid synthesis and quantification. Details about lipid synthesis and quantification are provided in Text S1 in the supplemental material.

SUPPLEMENTAL MATERIAL

Supplemental material for this article may be found at http://mbio.asm.org /lookup/suppl/doi:10.1128/mBio.00939-13/-/DCSupplemental.

Figure S1, DOCX file, 1.4 MB.
Figure S2, DOCX file, 0.2 MB.
Figure S3, DOCX file, 2.7 MB.
Table S1, DOCX file, 0.1 MB.
Text S1, DOCX file, 0.1 MB.

REFERENCES

1. **Hoiczyk E, Ring MW, McHugh CA, Schwär G, Bode E, Krug D, Altmeyer MO, Lu JZ, Bode HB.** 2009. Lipid body formation plays a central role in cell fate determination during developmental differentiation of *Myxococcus xanthus*. Mol. Microbiol. **74**:497–517. http:// dx.doi.org/10.1111/j.1365-2958.2009.06879.x.
2. **Ring MW, Schwär G, Thiel V, Dickschat JS, Kroppenstedt RM, Schulz S, Bode HB.** 2006. Novel iso-branched ether lipids as specific markers of developmental sporulation in the myxobacterium *Myxococcus xanthus*. J. Biol. Chem. **281**:36691–36700. http://dx.doi.org/10.1074/ jbc.M607616200.
3. **Manoil C, Kaiser D.** 1980. Guanosine pentaphosphate and guanosine tetraphosphate accumulation and induction of *Myxococcus xanthus* fruiting body development. J. Bacteriol. **141**:305–315.
4. **Manoil C, Kaiser D.** 1980. Accumulation of guanosine tetraphosphate and guanosine pentaphosphate in *Myxococcus xanthus* during starvation and myxospore formation. J. Bacteriol. **141**:297–304.
5. **O'Connor KA, Zusman DR.** 1991. Development in *Myxococcus xanthus* involves differentiation into two cell types, peripheral rods and spores. J. Bacteriol. **173**:3318–3333.
6. **Nariya H, Inouye M.** 2008. MazF, an mRNA interferase, mediates pro-

grammed cell death during multicellular *Myxococcus* development. Cell **132:**55–66. http://dx.doi.org/10.1016/j.cell.2007.11.044.

7. **Wireman JW, Dworkin M.** 1975. Morphogenesis and developmental interactions in myxobacteria. Science **189:**516–523. http://dx.doi.org/10.1126/science.806967.

8. **Shimkets LJ.** 1986. Role of cell cohesion in *Myxococcus xanthus* fruiting body formation. J. Bacteriol. **166:**842–848.

9. **Boynton TO, McMurry JL, Shimkets LJ.** 2013. Characterization of *Myxococcus xanthus* MazF and implications for a new point of regulation. Mol. Microbiol. **87:**1267–1276. http://dx.doi.org/10.1111/mmi.12165.

10. **Lee B, Holkenbrink C, Treuner-Lange A, Higgs PI.** 2012. *Myxococcus xanthus* developmental cell fate production: heterogeneous accumulation of developmental regulatory proteins and reexamination of the role of MazF in developmental lysis. J. Bacteriol. **194:**3058–3068. http://dx.doi.org/10.1128/JB.06756-11.

11. **Shimkets LJ.** 1999. Intercellular signaling during fruiting-body development of *Myxococcus xanthus*. Annu. Rev. Microbiol. **53:**525–549. http://dx.doi.org/10.1146/annurev.micro.53.1.525.

12. **Toal DR, Clifton SW, Roe BA, Downard J.** 1995. The *esg* locus of *Myxococcus xanthus* encodes the E1 alpha and E1 beta subunits of a branched-chain keto acid dehydrogenase. Mol. Microbiol. **16:**177–189. http://dx.doi.org/10.1111/j.1365-2958.1995.tb02291.x.

13. **Bode HB, Ring MW, Schwär G, Kroppenstedt RM, Kaiser D, Müller R.** 2006. 3-Hydroxy-3-methylglutaryl-coenzyme A (CoA) synthase is involved in biosynthesis of isovaleryl-CoA in the myxobacterium *Myxococcus xanthus* during fruiting body formation. J. Bacteriol. **188:**6524–6528. http://dx.doi.org/10.1128/JB.00825-06.

14. **Bode HB, Ring MW, Schwär G, Altmeyer MO, Kegler C, Jose IR, Singer M, Müller R.** 2009. Identification of additional players in the alternative biosynthesis pathway to isovaleryl-CoA in the myxobacterium *Myxococcus xanthus*. Chembiochem **10:**128–140. http://dx.doi.org/10.1002/cbic.200800219.

15. **Li Y, Luxenburger E, Müller R.** 2013. An alternative isovaleryl CoA biosynthetic pathway involving a previously unknown 3-methylglutaconyl CoA decarboxylase. Angew. Chem. Int. Ed. Engl. **52:**1304–1308. http://dx.doi.org/10.1002/anie.201207984.

16. **Downard J, Ramaswamy SV, Kil KS.** 1993. Identification of *esg*, a genetic locus involved in cell-cell signaling during *Myxococcus xanthus* development. J. Bacteriol. **175:**7762–7770.

17. **Downard J, Toal D.** 1995. Branched-chain fatty acids: the case for a novel form of cell-cell signalling during *Myxococcus xanthus* development. Mol. Microbiol. **16:**171–175. http://dx.doi.org/10.1111/j.1365-2958.1995.tb02290.x.

18. **Bode HB, Ring MW, Kaiser D, David AC, Kroppenstedt RM, Schwär G.** 2006. Straight-chain fatty acids are dispensable in the myxobacterium *Myxococcus xanthus* for vegetative growth and fruiting body formation. J. Bacteriol. **188:**5632–5634. http://dx.doi.org/10.1128/JB.00438-06.

19. **Hamilton JG, Comai K.** 1988. Rapid separation of neutral lipids, free fatty acids and polar lipids using prepacked silica Sep-Pak columns. Lipids **23:**1146–1149. http://dx.doi.org/10.1007/BF02535281.

20. **Kaiser D, Crosby C.** 1983. Cell movement and its coordination in swarms of *Myxococcus xanthus*. Cell Motil. **3:**227–245.

21. **Kearns DB, Venot A, Bonner PJ, Stevens B, Boons GJ, Shimkets LJ.** 2001. Identification of a developmental chemoattractant in *Myxococcus xanthus* through metabolic engineering. Proc. Natl. Acad. Sci. U. S. A. **98:**13990–13994. http://dx.doi.org/10.1073/pnas.251484598.

22. **Shi X, Wegener-Feldbrügge S, Huntley S, Hamann N, Hedderich R, Søgaard-Andersen L.** 2008. Bioinformatics and experimental analysis of proteins of two-component systems in *Myxococcus xanthus*. J. Bacteriol. **190:**613–624. http://dx.doi.org/10.1128/JB.01502-07.

23. **Kroos L, Kaiser D.** 1987. Expression of many developmentally regulated genes in *Myxococcus* depends on a sequence of cell interactions. Genes Dev. **1:**840–854. http://dx.doi.org/10.1101/gad.1.8.840.

24. **Fisseha M, Gloudemans M, Gill RE, Kroos L.** 1996. Characterization of the regulatory region of a cell interaction-dependent gene in *Myxococcus xanthus*. J. Bacteriol. **178:**2539–2550.

25. **Viswanathan P, Kroos L.** 2003. Cis elements necessary for developmental expression of a *Myxococcus xanthus* gene that depends on C signaling. J. Bacteriol. **185:**1405–1414. http://dx.doi.org/10.1128/JB.185.4.1405-1414.2003.

26. **Voelz H, Dworkin M.** 1962. Fine structure of *Myxococcus xanthus* during morphogenesis. J. Bacteriol. **84:**943–952.

27. **Kahnt J, Aguiluz K, Koch J, Treuner-Lange A, Konovalova A, Huntley S, Hoppert M, Søgaard-Andersen L, Hedderich R.** 2010. Profiling the outer membrane proteome during growth and development of the social bacterium *Myxococcus xanthus* by selective biotinylation and analyses of outer membrane vesicles. J. Proteome Res. **9:**5197–5208. http://dx.doi.org/10.1021/pr1004983.

28. **Pathak DT, Wei X, Bucuvalas A, Haft DH, Gerloff DL, Wall D.** 2012. Cell contact-dependent outer membrane exchange in myxobacteria: genetic determinants and mechanism. PLoS Genet. **8:**e1002626. http://dx.doi.org/10.1371/journal.pgen.1002626.

29. **Wei X, Pathak DT, Wall D.** 2011. Heterologous protein transfer within structured myxobacteria biofilms. Mol. Microbiol. **81:**315–326. http://dx.doi.org/10.1111/j.1365-2958.2011.07710.x.

30. **Lancero H, Brofft JE, Downard J, Birren BW, Nusbaum C, Naylor J, Shi W, Shimkets LJ.** 2002. Mapping of *Myxococcus xanthus* social motility *dsp* mutations to the *dif* genes. J. Bacteriol. **184:**1462–1465. http://dx.doi.org/10.1128/JB.184.5.1462-1465.2002.

31. **Wältermann M, Hinz A, Robenek H, Troyer D, Reichelt R, Malkus U, Galla HJ, Kalscheuer R, Stöveken T, von Landenberg P, Steinbüchel A.** 2005. Mechanism of lipid-body formation in prokaryotes: how bacteria fatten up. Mol. Microbiol. **55:**750–763. http://dx.doi.org/10.1111/j.1365-2958.2004.04441.x.

32. **Orndorff PE, Dworkin M.** 1980. Separation and properties of the cytoplasmic and outer membranes of vegetative cells of *Myxococcus xanthus*. J. Bacteriol. **141:**914–927.

33. **Bui NK, Gray J, Schwarz H, Schumann P, Blanot D, Vollmer W.** 2009. The peptidoglycan sacculus of *Myxococcus xanthus* has unusual structural features and is degraded during glycerol-induced myxospore development. J. Bacteriol. **191:**494–505. http://dx.doi.org/10.1128/JB.00608-08.

34. **Nudleman E, Wall D, Kaiser D.** 2005. Cell-to-cell transfer of bacterial outer membrane lipoproteins. Science **309:**125–127. http://dx.doi.org/10.1126/science.1112440.